Bioorganic & Medicinal Chemistry xxx (2016) xxx–xxx

Contents lists available at ScienceDirect

Bioorganic & Medicinal Chemistry

journal homepage: www.elsevier.com/locate/bmc

Synthesis and antitumor activity evaluation of a novel combi-nitrosourea prodrug: Designed to release a DNA cross-linking agent and an inhibitor of O^6-alkylguanine-DNA alkyltransferase

Guohui Sun, Na Zhang, Lijiao Zhao *, Tengjiao Fan, Shufen Zhang, Rugang Zhong

Beijing Key Laboratory of Environmental & Viral Oncology, College of Life Science and Bioengineering, Beijing University of Technology, Beijing 100124, PR China

ARTICLE INFO

Article history:
Received 5 February 2016
Revised 22 March 2016
Accepted 25 March 2016
Available online xxxx

Keywords:
Combi-nitrosourea
O^6-alkylguanine-DNA alkyltransferase
dG–dC cross-links
Drug resistance
Cytotoxicity

ABSTRACT

The drug resistance of CENUs induced by O^6-alkylguanine-DNA alkyltransferase (AGT), which repairs the O^6-alkylated guanine and subsequently inhibits the formation of dG–dC cross-links, hinders the application of CENU chemotherapies. Therefore, the discovery of CENU analogs with AGT inhibiting activity is a promising approach leading to novel CENU chemotherapies with high therapeutic index. In this study, a new combi-nitrosourea prodrug 3-(3-(((2-amino-9H-purin-6-yl)oxy)methyl)benzyl)-1-(2-chloroethyl)-1-nitrosourea (**6**), designed to release a DNA cross-linking agent and an inhibitor of AGT, was synthesized and evaluated for its antitumor activity and ability to induce DNA interstrand cross-links (ICLs). The results indicated that **6** exhibited higher cytotoxicity against mer$^+$ glioma cells compared with ACNU, BCNU, and their respective combinations with O^6-benzylguanine (O^6-BG). Quantifications of dG–dC cross-links induced by **6** were performed using HPLC–ESI-MS/MS. Higher levels of dG–dC cross-link were observed in **6**-treated human glioma SF763 cells (mer$^+$), whereas lower levels of dG–dC cross-link were observed in **6**-treated calf thymus DNA, when compared with the groups treated with BCNU and ACNU. The results suggested that the superiority of **6** might result from the AGT inhibitory moiety, which specifically functions in cells with AGT activity. Molecular docking studies indicated that five hydrogen bonds were formed between the O^6-BG analogs released from **6** and the five residues in the active pocket of AGT, which provided a reasonable explanation for the higher AGT-inhibitory activity of **6** than O^6-BG.

1. Introduction

Chloroethylnitrosoureas (CENUs), such as 1-[(4-amino-2-methyl-5-pyrimidinyl)-methyl]-3-(2-chloroethyl)-3-nitrosourea (ACNU), 1,3-bis(2-chloroethyl)-1-nitrosourea (BCNU), 1-(2-chloroethyl)-3-cyclohexyl-1-nitrosourea (CCNU), and 1-(2-chloroethyl)-3-(4-methylcyclohexyl)-1-nitrosourea (me-CCNU) (Fig. 1), are an important type of bifunctional alkylating agents widely used for the clinical treatment of cancer.[1–4] They are highly effective for the treatment of brain tumors due to their ability to penetrate the blood–brain barrier.[1,2] Chloroethylation of the O^6-position in DNA guanine residues is the major source of the antitumor activity of CENUs because the O^6-chloroethylating adducts can result in the formation of dG–dC interstrand cross-links (ICLs), which can inhibit DNA double-strand separation during replication and transcription, leading to cell apoptosis if not repaired correctly.[5–9] As shown in Figure 2, CENUs can decompose under physiological conditions to produce a chloroethylating intermediate that attacks the deoxyguanosine (dGuo) to form O^6-(2-chloroethyl)deoxyguanosine (O^6-ClEtdGuo). Then O^6-ClEtdGuo undergoes intramolecular cyclization to yield N1,O^6-ethanodeoxyguanosine (N1,O^6-EtdGuo) followed by a second alkylation of the complementary deoxycytidine (dCyd) to produce an ethyl bridge between the N1 position of guanine and the N3 position of cytosine, resulting in the formation of a dG–dC cross-link.[1,2]

Abbreviations: CENUs, chloroethylnitrosoureas; ACNU, 1-[(4-amino-2-methyl-5-pyrimidinyl)methyl]-3-(2-chloroethyl)-3-nitrosourea; BCNU, 1,3-bis(2-chloroethyl)-1-nitrosourea; CCNU, 1-(2-chloroethyl)-3-cyclohexyl-1-nitrosourea; me-CCNU, 1-(2-chloroethyl)-3-(4-methyl-cyclohexyl)-1-nitrosourea; ICLs, interstrand cross-links; O^6-ClEtdGuo, O^6-(2-chloroethyl)deoxyguanosine; N1,O^6-EtdGuo, N1,O^6-ethanodeoxyguanosine; dGuo, deoxyguanosine; dCyd, deoxycytidine; AGT, O^6-alkylguanine-DNA alkyltransferase; Cys145, cysteine145; O^6-BG, O^6-benzylguanine; HPLC–ESI-MS/MS, high-performance liquid chromatography electrospray ionization tandem mass spectrometry; DMF, *N*,*N*-dimethylformamide; PBS, phosphate buffer saline; MEM-EBSS, minimum essential medium with Earle's balanced salts; FBS, fetal bovine serum; $t_{1/2}$, half-life; CT DNA, calf thymus DNA; PDB, Protein Data Bank; O^6-MG, O^6-methylguanine; RMSD, root mean square deviation; TLC, thin-layer chromatography; Hz, Hertz; HRMS, high-resolution mass spectrum; TEA, triethylamine; SD, standard deviation; CCK8, Cell Counting Kit-8; DMSO, dimethyl sulfoxide; DNase I, deoxyribonuclease I; ClAP, alkaline phosphatase; SRM, selected reaction monitoring.

* Corresponding author. Tel.: +86 10 67391667.
E-mail address: zhaolijiao@bjut.edu.cn (L. Zhao).

http://dx.doi.org/10.1016/j.bmc.2016.03.041
0968-0896/

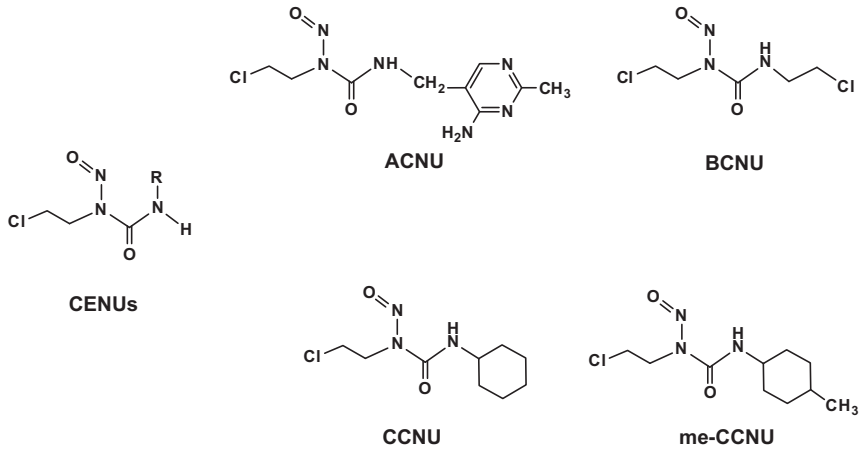

Figure 1. Typical CENUs used in the clinical treatment of cancer.

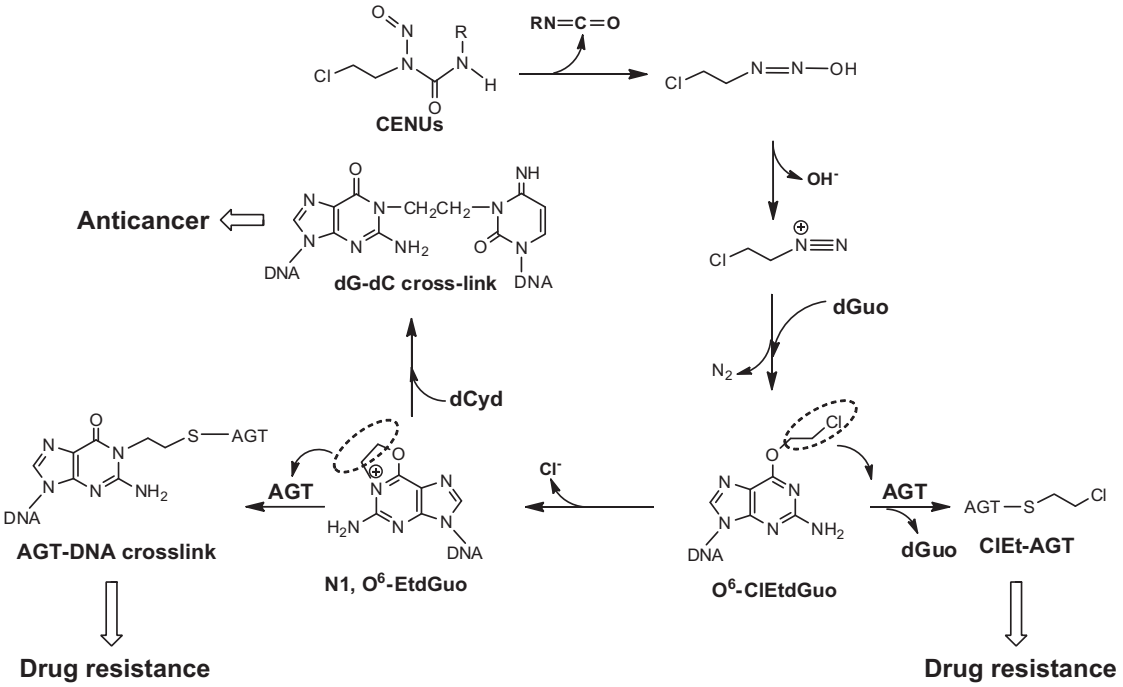

Figure 2. The general mechanisms for the formation and repair of dG–dC cross-links.

However, O^6-alkylguanine-DNA alkyltransferase (AGT) in tumor cells can repair the intermediate O^6-ClEtdGuo and N1,O^6-EtdGuo by transferring the O^6-position lesions to its own active site cysteine145 (Cys145) residue, thereby inhibiting the generation of lethal dG–dC cross-links and leading to drug resistance (Fig. 2).[10–15] After accepting the alkyl groups, AGT is rapidly degraded by ubiquitination-dependent proteolysis.[16,17] Based on the AGT levels, most human cell lines can be divided into two classes: cells with low or no AGT activity (termed mer^-), which are sensitive to the cytotoxic effects of CENUs and were observed to have high levels of ICLs, and cells with high levels of AGT (termed mer^+), which are resistant to these effects and exhibited low levels of ICLs.[5,18–22] Because high levels of AGT can cause a strong resistance to CENU chemotherapy in tumor cells, a series of AGT inhibitors were synthesized and were used as adjuvants to improve the chemotherapeutic effects of CENUs.[23–30] The potent inactivator O^6-benzylguanine (O^6-BG), which acts as a pseudosubstrate to form *S*-benzylcysteine at the active site of AGT to inactivate the protein, is currently undergoing clinical trials as an adjuvant in combination with BCNU.[31–34] Although O^6-BG is a promising AGT inhibitor, its modest inactivating ability and poor water solubility limit its clinical effectiveness.[15,27,29,30,33,34] The concept of using a 'combi-molecule' to overcome the drug resistance has been attempted. Qiu et al.[35,36] synthesized a series of combi-nitrosoureas with epidermal growth factor receptor tyrosine kinase inhibitory properties while maintaining DNA cross-linking reactivity.

In this study, we describe the synthesis, antitumor activity and mechanism of action of a new combi-nitrosourea prodrug 3-(3-(((2-amino-9H-purin-6-yl)oxy)methyl)benzyl)-1-(2-chloroethyl)-1-nitrosourea (**6**), which is designed to release a DNA cross-linking agent and an inhibitor of AGT (Scheme 1). This study is expected to provide a foundation for the development of novel CENU chemotherapies with high efficacy.

Please cite this article in press as: Sun, G.; et al. *Bioorg. Med. Chem.* (2016), http://dx.doi.org/10.1016/j.bmc.2016.03.041

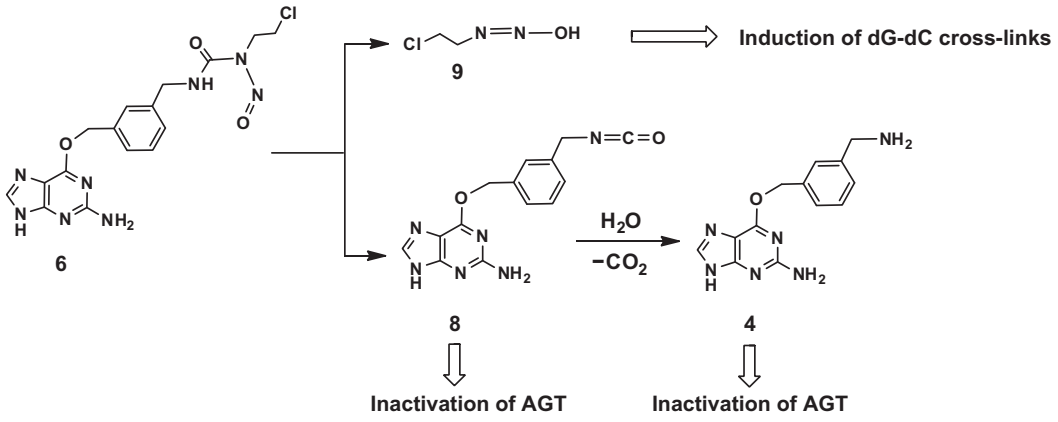

Scheme 1. The decomposition pathway of combi-chloroethylnitrosourea prodrug **6**.

2. Results and discussion

2.1. Chemistry

According to the results obtained from previously published studies,[30,37] the meta-substitution at the benzyl of O^6-BG can result in higher inhibitory activity against AGT than that of *ortho*- or *para*-substitution. Thus, the novel combi-nitrosourea prodrug **6** was synthesized and designed to release the meta-substituted O^6-BG analog 6-((3-(isocyanatomethyl)benzyl)oxy)-9H-purin-2-amine (**8**) and its hydrolysate meta-substituted O^6-BG analog O^6-[3-(aminomethyl)benzyl]guanine (**4**) as an AGT inhibitor, along with chloroethylating intermediate **9**, which can induce dG–dC cross-links. The synthesis of **6** is shown in Scheme 2. Briefly, 1-(2-amino-9H-purin-6-yl)-1-methylpyrrolidinium chloride (**2**) was prepared by the reaction of 2-amino-6-chloroguanine (**1**) with *N*-methylpyrrolidine in anhydrous *N*,*N*-dimethylformamide (DMF) at room temperature. Then, **2** was condensed with 2,2,2-trifluoro-*N*-(3-(hydroxymethyl)benzyl)-acetamide (**7**) under argon atmosphere to give *N*-(3-(((2-amino-9H-purin-6-yl)oxy)methyl) benzyl)-2,2,2-trifluoroacetamide (**3**) in the presence of potassium *t*-butoxide. The trifluoroacetyl protecting group of intermediate **3** was removed by refluxing in the presence of a methanol/water solution to give O^6-[3-(aminomethyl)benzyl]guanine (**4**). The reaction of **4** with 2-chloroethyl isocyanate in anhydrous DMF yielded 1-(3-(((2-amino-9H-purin-6-yl)oxy)-methyl)benzyl)-3-(2-chloroethyl)urea (**5**) followed by nitrosation with nitrosonium tetrafluoroborate in acetonitrile containing a moderate amount of glacial acetic acid at 0 °C to afford the desired final product **6**.

2.2. Stability

The degradation of **6** was monitored by HPLC-UV analysis in phosphate buffer saline (PBS) and in minimum essential medium with Earle's balanced salts (MEM-EBSS) supplemented with 10% fetal bovine serum (FBS) and antibiotics (100 U/mL penicillin and 100 μg/mL streptomycin). The stability study suggested that **6** has similar decomposition properties with classical CENUs. As shown in Figure 3, the half-lives ($t_{1/2}$) of **6** in PBS and MEM-EBSS were approximately 30 min and 18 min, respectively. The $t_{1/2}$

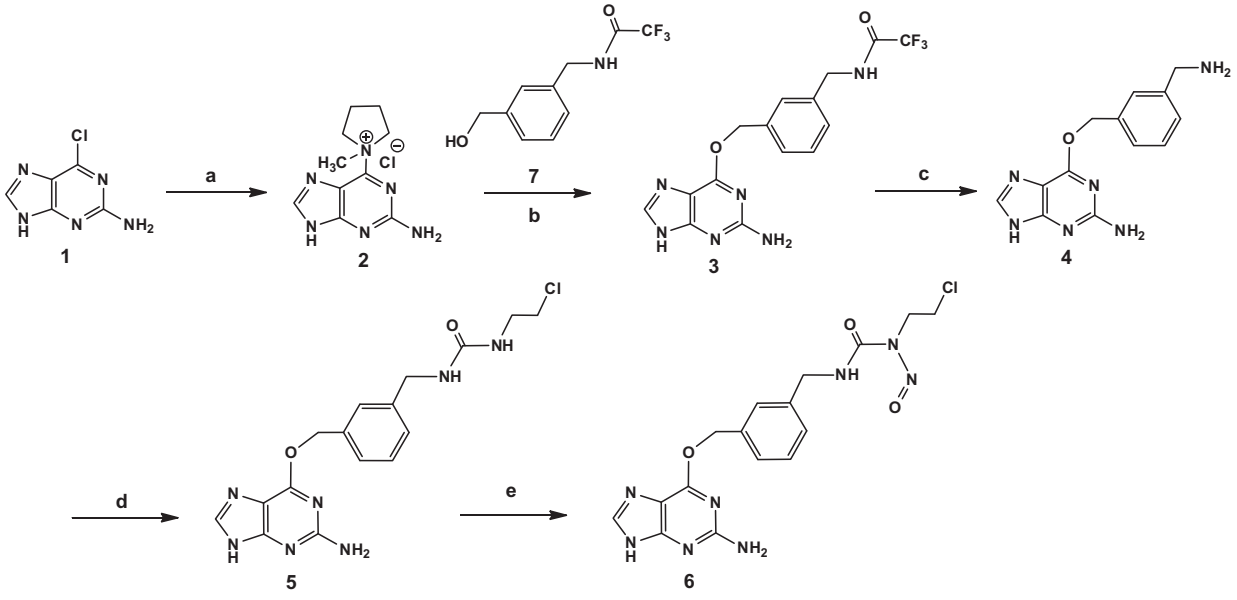

Scheme 2. Synthesis of the combi-nitrosourea prodrug **6**[a]. [a]Reagents and conditions: (a) (1) *N*-methylpyrrolidine, DMF, room temperature, 18 h; (2) addition of acetone to complete precipitation. (b) (1) Potassium *t*-butoxide, DMF, argon atmosphere, room temperature, 4 h; (2) addition of glacial acetic acid to neutralize excess potassium *t*-butoxide. (c) Potassium carbonate, methanol/water (17:1), reflux, 2 h. (d) 2-Chloroethyl isocyanate, DMF, 0 °C to room temperature, 2 h. (e) Nitrosonium tetrafluoroborate, acetonitrile, glacial acetic acid, 0 °C, 3 h.

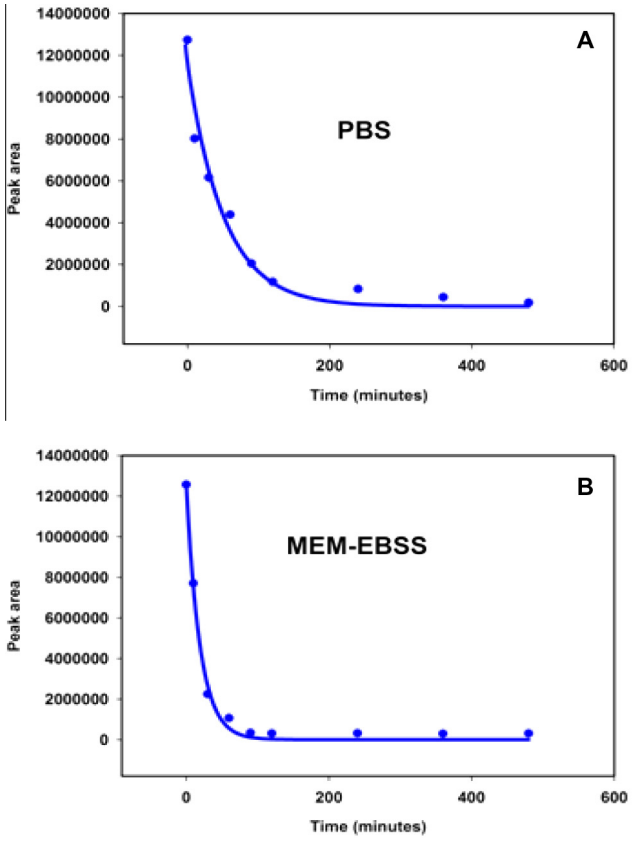

Figure 3. The degradation of **6** performed in (A) PBS and (B) MEM-EBSS over an 8 h incubation.

was similar to that of 15 min of BCNU in serum-containing medium.[38] The degradation of **6** was accompanied by the generation of a main peak containing **8** and a minor peak containing **4** (see Fig. S1A in the Supplementary materials). The two products were both monitored by MS/MS with the transitions of *m*/*z* 271 → 254 for **4** and *m*/*z* 297 → 254 for **8** (see Fig. S1B in the Supplementary materials). This is also supported by the general decomposition pathway described previously, which indicated that chloroethyl-diazohydroxide, isocyanate and amine generated from hydrolysis of isocyanate were the main decomposition products of CENUs.[1,2,38]

2.3. Sensitivity of human glioma cells to 6

To demonstrate the efficacy of the dual functions of the combi-chloroethylnitrosourea prodrug, **6** was tested in a cell survival assay against three human glioma cells with different AGT activities, namely, SF126 (mer^-, little or no AGT activity), SF767 (mer^+, 61 fmol/10^6 cells) and SF763 (mer^+, 119 fmol/10^6 cells).[39,40] The cytotoxic effects of **6** were compared with ACNU, BCNU and the combination of ACNU or BCNU with O^6-BG (Fig. 4). As shown in Figure 4A and B, **6** (IC_{50} = 50 μM) was >6-fold more cytotoxic than ACNU (IC_{50} = 320 μM) and its combination with O^6-BG (IC_{50} = 310 μM) against SF126 cells, while it exhibited lower toxicity than BCNU (IC_{50} = 20 μM) alone and its combination with O^6-BG (IC_{50} = 25 μM). For SF767 cells, which express moderate levels of AGT, **6** (IC_{50} = 25 μM) exhibited significantly higher cytotoxicity than ACNU alone (IC_{50} = 500 μM) and its combination with O^6-BG (IC_{50} = 400 μM) (Fig. 4C), and exhibited a slightly higher toxicity than BCNU alone (IC_{50} = 45 μM) and the combination of BCNU with O^6-BG (IC_{50} = 30 μM) (Fig. 4D). Compound **6** was also tested in SF763 cells, which express high levels of AGT. The results showed that **6** (IC_{50} = 35 μM) was significantly more cytotoxic than ACNU (IC_{50} > 1000 μM), BCNU (IC_{50} = 100 μM) and their respective combinations with O^6-BG (1000 μM and 55 μM, respectively) (Fig. 4E and F). Considering the possible cytotoxicity of the final species decomposed from **6**, cell survival assays were performed by treating SF126, SF767 and SF763 cells with compound **4**. The result indicated that compound **4** was nontoxic to cell growth with a death rate below 3%.

The high sensitivity of SF767 and SF763 cells to **6** suggested that the AGT-mediated resistance was effectively weakened by exposure to **6**. The high cytotoxicity of **6** against mer^+ cells may be due to the inhibition of AGT activity by the inhibitor released from **6**, thereby enhancing the sensitivity of these cells to DNA cross-linking agent **9**. The chemosensitivity of cells to ACNU or BCNU largely depends on the levels of AGT, while the dependence was mostly deprived by **6**. In contrast, for SF126 cells (Fig. 4B), **6** exhibited higher IC_{50} compared with BCNU alone and its combination with O^6-BG, which may be due to the release of the highly cytotoxic 2-chloroethyl isocyanate from the decomposition of BCNU and the minimized function of **8** or **4** on low AGT-expressed SF126 cells. The lower cytotoxicity of **6** against SF126 cells compared with SF767 and SF763 cells indicated that the superiority of **6** could be specifically reflected in mer^+ cells.

2.4. Quantitation of dG–dC cross-links by HPLC–ESI-MS/MS analysis

On the basis of the hypothesis that the dG–dC cross-links may be used as an indicator for predicting the anticancer efficiency of CENUs, which was put forward in our previous studies,[41,42] we quantified the dG–dC cross-links induced by **6** using HPLC–ESI-MS/MS to explore the relationship between the levels of DNA cross-link and the cytotoxicity of **6**. The isotope dilution HPLC–ESI-MS/MS methodology has been validated for the quantitation of dG–dC cross-links in calf thymus DNA (CT DNA) and cells treated with CENUs, as described in our previous study.[22] The quantitative calibration curve was constructed by plotting the selected reaction monitoring (SRM) peak area ratio of dG–dC to $^{15}N_3$-dG–dC against the corresponding concentration ratio with a correlation coefficient (R^2) of 0.9999 (Fig. S2 in the Supplementary materials). The typical SRM ion chromatograms of dG–dC and $^{15}N_3$-dG–dC internal standard in the DNA enzymatic hydrolysates are shown in Figure 5. The peak corresponding to dG–dC was coeluted with $^{15}N_3$-dG–dC internal standard with a retention time of approximately 11.24 min. No signal of dG–dC cross-links was detected in the control CT DNA or in the control cell samples, suggesting no interference or contamination in the analyte channels from the internal standard or enzymatic hydrolysates.

CT DNA was treated with different concentrations of **6** (0.1, 0.2, and 0.4 mM) for 12 h. As shown in Figure 6A (data listed in Table S1 in the Supplementary materials), the formation of dG–dC cross-links was concentration dependent. The levels of dG–dC cross-link in CT DNA treated with **6** were lower than those of ACNU and BCNU over the tested concentration range. However, the levels of dG–dC cross-link in human glioma SF763 cells (Fig. 6B, data listed in Table S2 in the Supplementary materials) induced by **6** were significantly higher than those of ACNU and BCNU over the same concentration range as described with CT DNA. These combined results indicate that the increased levels of dG–dC cross-link in SF763 cells after exposure to **6** were due to the inhibition of AGT activity by O^6-BG analogs **8** and its hydrolytic product **4** released from the decomposition of **6**. In contrast, the decreased levels of dG–dC cross-link in CT DNA treated with **6** may result from the invalidation of **8** and **4** in the absence of AGT in vitro.

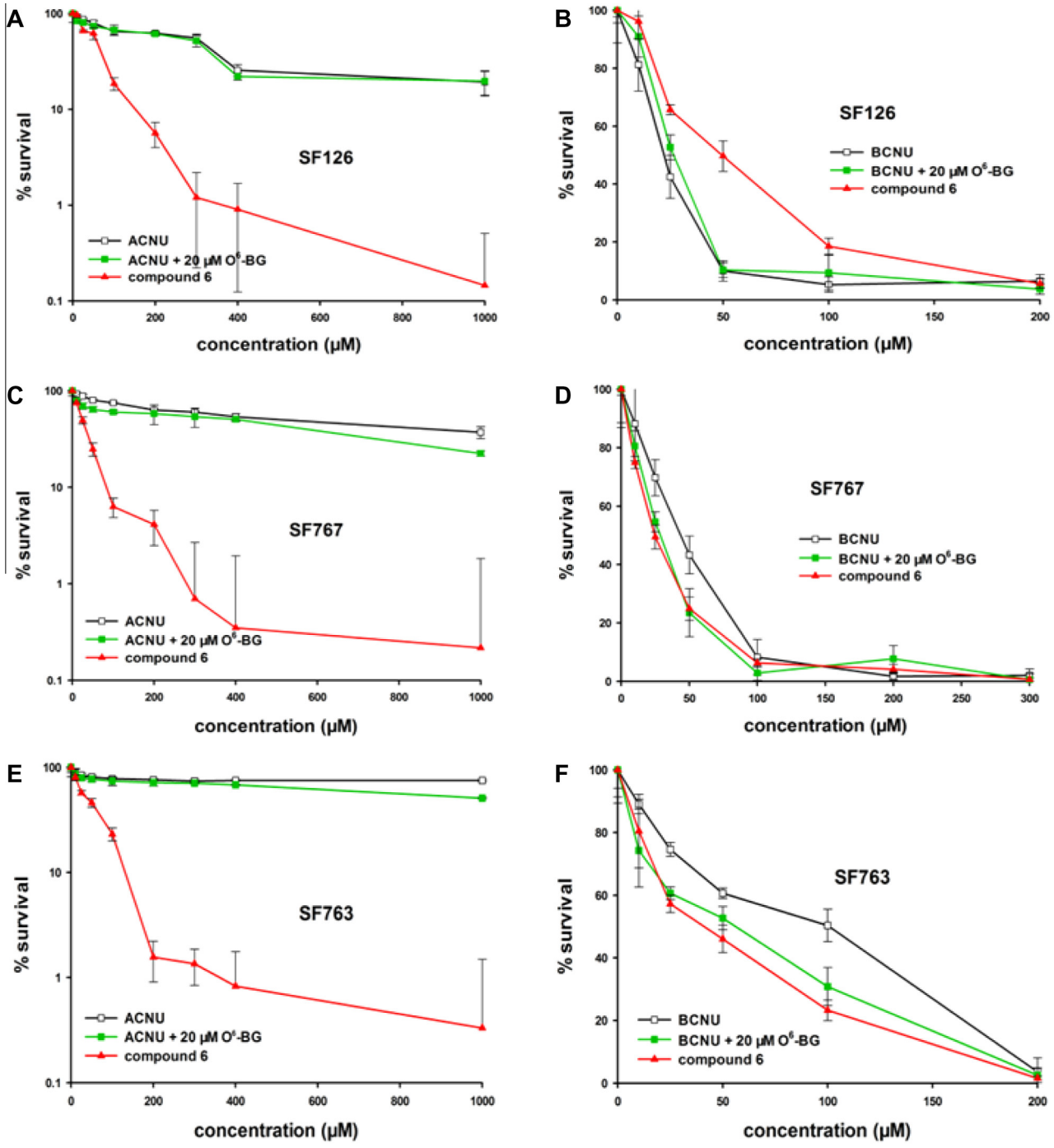

Figure 4. Cell survival curves for human glioma SF126, SF767 and SF763 cells treated with the indicated drugs with various concentrations. (A) SF126 cells treated with ACNU, ACNU combined with 20 μM O^6-BG, and **6**; (B) SF126 cells treated with BCNU, BCNU combined with 20 μM O^6-BG, and **6**; (C) SF767 cells treated with ACNU, ACNU combined with 20 μM O^6-BG, and **6**; (D) SF767 cells treated with BCNU, BCNU combined with 20 μM O^6-BG, and **6**; (E) SF763 cells treated with ACNU, ACNU combined with 20 μM O^6-BG, and **6**; and (F) SF763 cells treated with BCNU, BCNU combined with 20 μM O^6-BG, and **6**. The black open square, green square and red triangle represent the treatments with ACNU or BCNU alone, combination treatments of ACNU or BCNU with 20 μM O^6-BG, and treatments with **6**, respectively.

2.5. Molecular docking of human AGT inhibitors

The molecular structure of AGT used for docking studies was acquired from homology modeling using Protein Data Bank (PDB) entry 1T39 (3.3 Å resolution) and 1QNT (1.90 Å resolution) as templates. To validate the GOLD docking method employed in this study, self-docking was performed using the human AGT with PDB entry 1T38 (3.2 Å resolution) bound to DNA containing O^6-methylguanine (O^6-MG) as the protein–ligand crystal complex model. The DNA duplex in the DNA–AGT complex was removed except for O^6-MG, which was used as a native ligand for self-docking, and solvent molecules were deleted in the protein crystal structure of 1T38. The root mean square deviation (RMSD) of the ligand position between the docked pose with highest fitness score and the pose in protein–ligand crystal complex was 0.0882 Å (Fig. 7A). Therefore, the docking conformation produced by GOLD

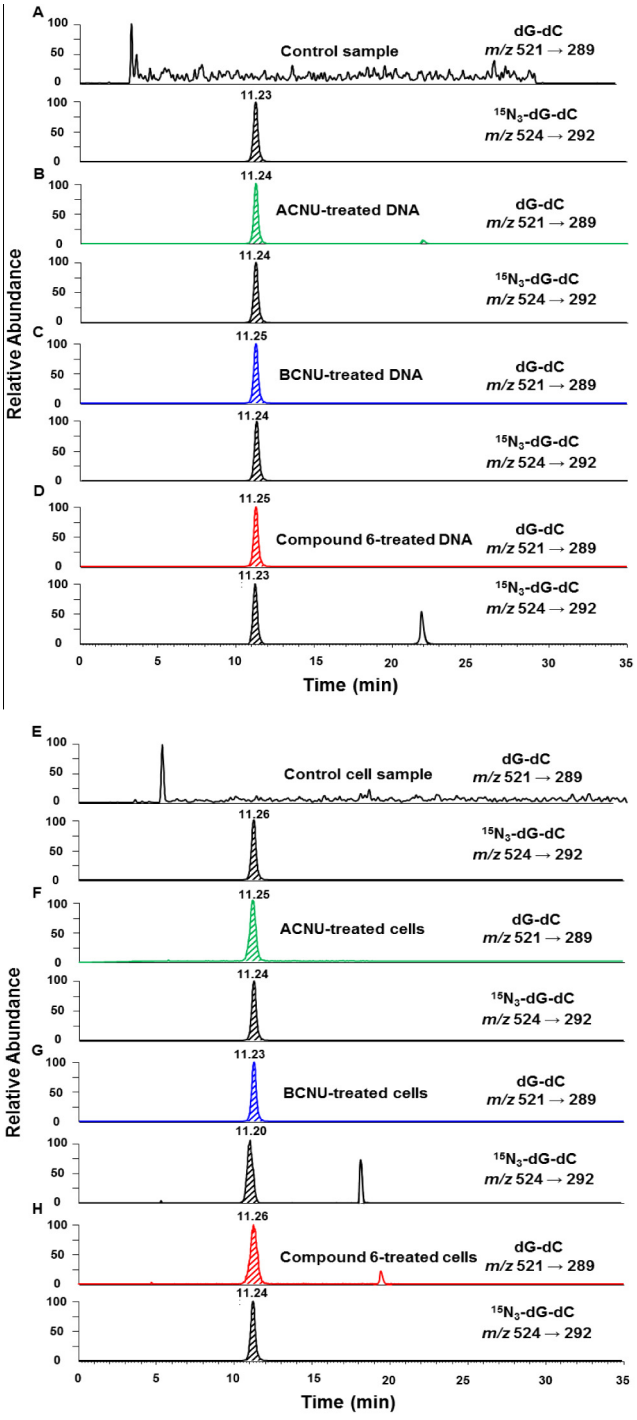

Figure 5. Typical SRM ion chromatograms of dG–dC and $^{15}N_3$-dG–dC internal standard in the DNA enzymatic hydrolysates from (A) control CT DNA sample; (B) ACNU-treated CT DNA; (C) BCNU-treated CT DNA; (D) compound **6**-treated CT DNA; (E) control cell sample; (F) ACNU-treated cells; (G) BCNU-treated cells; and (H) compound **6**-treated cells.

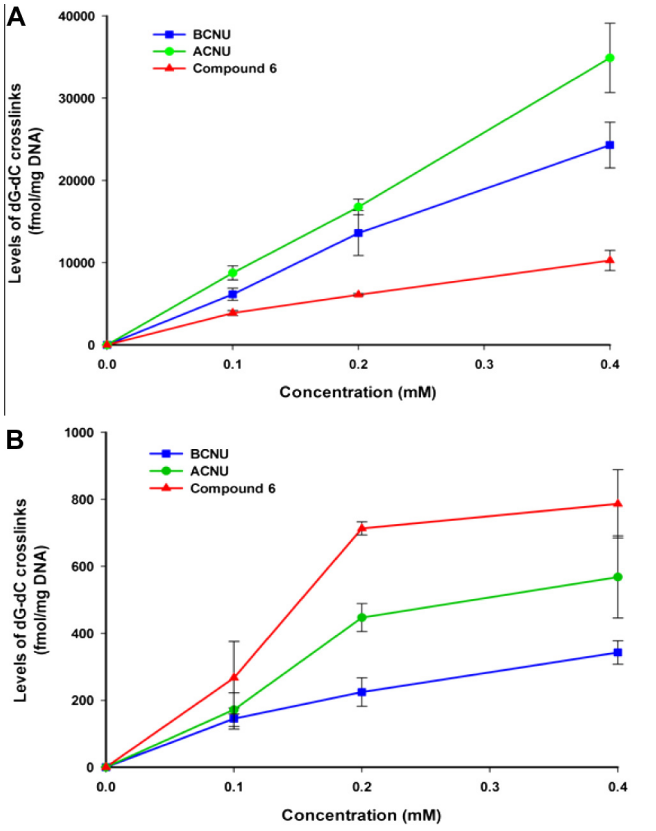

Figure 6. The levels of dG–dC cross-link in CT DNA (A) or SF763 cells (B) treated with ACNU (green circle), BCNU (blue square), and **6** (red triangle).

was similar to the crystal structure. This suggests that GOLD is suitable for performing the docking of AGT with the corresponding inhibitors.

Fig. 7B shows the key hydrogen bonding interaction of O^6-BG with the active pocket of AGT. Four hydrogen bonds were formed between O^6-BG and Try114, Cys145, Val148 and Ser159, which is supported by the results of previous studies.[41] The interaction of **8** and **4** with the active pocket of AGT is shown in Fig. 7C and D, respectively. Five specific hydrogen bonds were observed between five residues and **8** or **4**. Two new hydrogen-bonding interactions were formed between Asn157 and the N3 position of guanine and between Tyr158 and the isocyanate group of **8**, although the loss of a hydrogen bond formed between Val148 and the 2-amino group of guanine was observed in the docked pose of **8** compared with that of O^6-BG. Moreover, compound **4** can also result in the formation of a new hydrogen bond between the aminomethyl group and Asn137, except for the four residues (Try114, Cys145, Val148, and Ser159) also formed in the complex of AGT with O^6-BG. Thus, the additional interactions in the active site pocket may increase the affinity of **8** or **4** binding to AGT and contribute to the enhanced AGT inhibitory activity when compared with O^6-BG. Pauly et al. has demonstrated that compound **4** exhibited better AGT inhibitory activity than O^6-BG.[30] This result provides a plausible explanation for the superior cytotoxicity of **6** compared with the combination of ACNU or BCNU with O^6-BG in cells with high AGT expression and for the high levels of dG–dC cross-link in cells treated with **6**.

3. Conclusions

In this study, a new combi-nitrosourea **6**, which is designed to simultaneously release a DNA cross-linking agent and an inhibitor of AGT, was synthesized and evaluated for antitumor activity. The survival assay indicated that **6** exhibited more potency against mer^+ tumor cells than the clinically widely used ACNU and BCNU. Especially, **6** was more effective in inhibiting mer^+ tumor cells growth than the combination of ACNU or BCNU with O^6-BG. On the basis of the hypothesis that the dG–dC cross-links may be used as an indicator for predicting the anticancer efficiency of CENUs, we quantified the dG–dC cross-links induced by **6** using

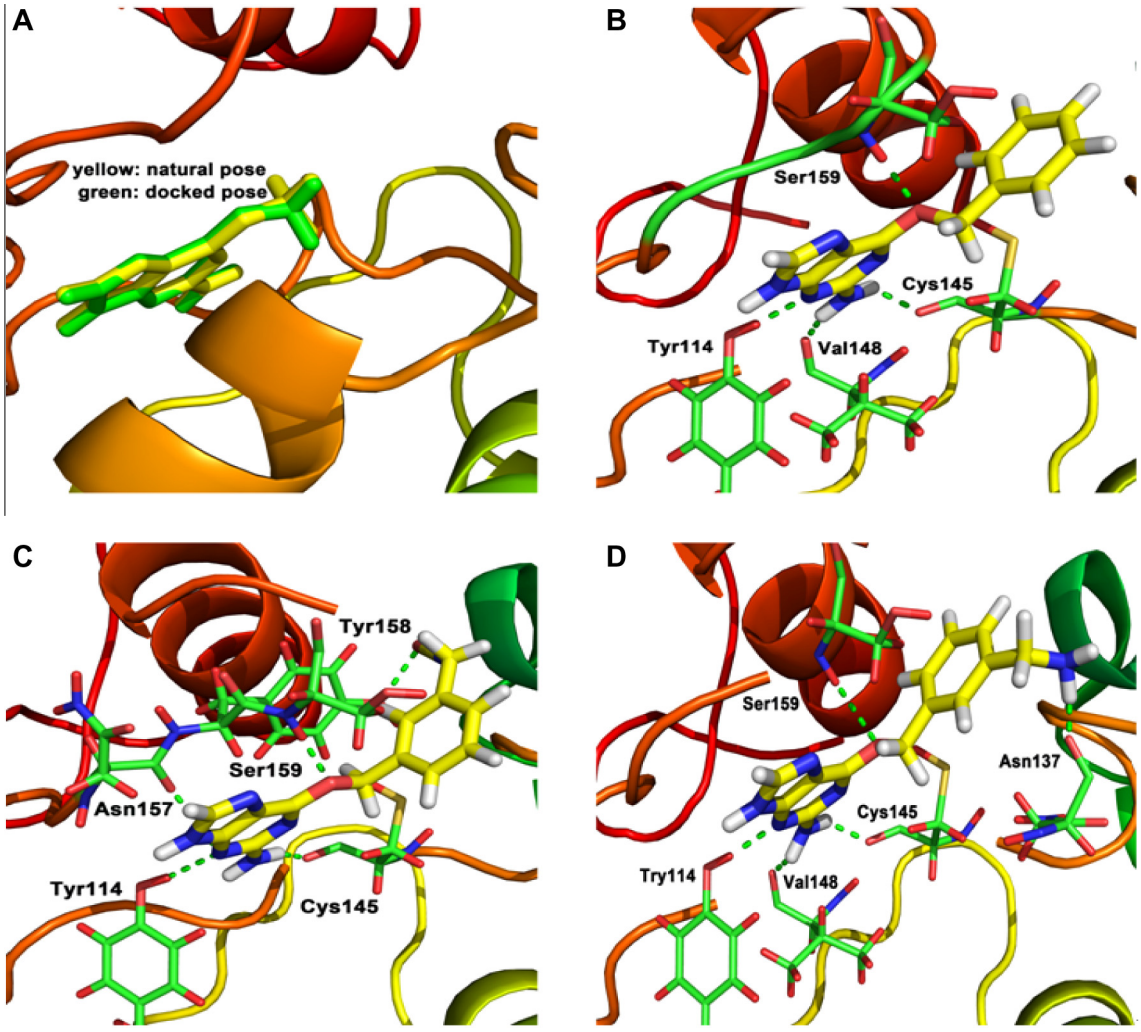

Figure 7. (A) Overlap of the ligand between the docked pose with the highest fitness score and the pose in the protein–ligand crystal complex; The key hydrogen bonding interactions between O^6-BG (B) or **8** (C) or **4** (D) and the amino acid residues in the active pocket of AGT. The residues forming hydrogen bonds are presented in the line model with green representing carbon atoms. O^6-BG, **8** and **4** are present in the stick model with yellow representing carbon atoms. The remaining protein is displayed in the cartoon model.

HPLC–ESI-MS/MS to explore the relationship between the levels of DNA cross-link and the cytotoxicity of **6**. Higher levels of dG–dC cross-link were observed in human glioma SF763 cells treated with **6** compared with cells treated with ACNU or BCNU, while the dG–dC cross-links were observed at lower levels in CT DNA treated with **6** than those treated with ACNU or BCNU. These combined results suggest that the superiority of **6** may result from the AGT inhibitory moiety, which specifically functions in mer^+ cells. In addition, the superior antitumor activity and DNA cross-linking ability of **6** were explained by molecular docking studies. Although **6** has slightly better water solubility than O^6-BG and exhibited preferable activity compared with the traditional CENU chemotherapies against mer^+ cells, the non-selectivity to tumor cells are likely to be a potential disadvantage hampering the further investigations of **6** in animal experiments and clinical studies. Therefore, we are working on the development of **6** analogs with higher water solubility and targeting to cancer cells.

4. Experimental section

4.1. Chemistry

All of the chemicals, solvents, reagents, and enzymes were purchased from Sigma–Aldrich Chemical Co. (Milwaukee, WI, USA), J&K Scientific Ltd. (Shanghai, China), Beijing Chemicals Co. (Beijing, China), and TaKaRa Biotech (Tokyo, Japan) and were used without further purification. The dG–dC cross-link standard and isotope-labeled $^{15}N_3$-dG–dC internal standard were prepared as previously described.[43,44] All of the melting points were measured with a XT4A Electrothermal melting point apparatus and were reported as uncorrected values. Argon was used for inert atmosphere operations in flame-dried glassware. Thin-layer chromatography (TLC) was performed on silica gel F-254 TLC plates. Column chromatography was performed using silica gel (200–300 mesh) with the solvent mixtures specified in the corresponding experiment. ^1H and ^{13}C NMR spectra were recorded on a Bruker AV 400 M spectrometer (400 MHz ^1H frequency and 100 MHz ^{13}C frequency). Chemical shifts are reported as δ (ppm) relative to tetramethylsilane as an internal standard, and the coupling constants (J) are reported in Hertz (Hz). IR spectra were recorded using KBr pellets on a Bruker Vertex 70FT-IR spectrophotometer. ESI-MS spectra were performed on a Thermo TSQ Quantum Discovery MAX triple quadrupole mass spectrometer (Thermo Finnigan, San Jose, CA). High-resolution mass spectra (HRMS) were obtained using a Bruker maXis UHR-TOF mass spectrometer (Bruker Daltonics, Bremen, Germany). HPLC-UV analysis was conducted on a Thermo Finnigan HPLC system (Thermo Finnigan, San Jose, CA) interfaced with a diode array detector and an autosampler.

The syntheses of compounds **2**–**4** and **7** were performed as previously described with some modifications.[30]

4.1.1. 1-(2-Amino-9H-purin-6-yl)-1-methylpyrrolidinium chloride (2)

This compound was prepared as previously described by Keppler et al.[45] To a solution of 2-amino-6-chloroguanine (1.0 g, 5.9 mmol) in 40 mL anhydrous DMF at room temperature was added 1.4 mL *N*-methylpyrrolidine (13.2 mmol), and the reaction mixture was stirred for 18 h, followed by the addition of 2 mL acetone to complete precipitation. The precipitates were collected on a filter and washed twice with ether, then dried in vacuo to give 0.9 g compound **2** (3.5 mmol, yield 59%) as a white solid. Mp 200–202 °C. ^{1}H NMR (DMSO-d_6) δ: 2.05–2.50 (m, 4H, –CH_2-CH_2–), 3.65 (s, 3H, –CH_3), 3.95–4.61 (m, 4H, –CH_2-N$^+$(CH_3)-CH_2–), 7.11 (s, 2H, –NH_2), 8.35 (s, 1H, H8), 13.44 (s, 1H, H9) ppm. ^{13}C NMR (100 MHz, DMSO-d_6) δ: 159.5, 159.03, 152.1, 143.1, 116.5, 64.6, 56.5, 52.1, 21.9, 19.0. IR (KBr): 3364, 3288, 3188, 1634 cm^{-1}. MS (ESI): *m*/*z* (M−Cl)$^+$ 219.1. HRMS (ESI): *m*/*z* calcd for $C_{10}H_{15}N_6Cl$ (M−Cl)$^+$ 219.1358, found 219.1362.

4.1.2. 2,2,2-Trifluoro-*N*-(3-(hydroxymethyl)benzyl)acetamide (7)

To a solution of 4-(aminomethyl)-benzyl alcohol hydrochloride (2.2 g, 12.6 mmol) in 15 mL anhydrous methanol was added 1.7 mL triethylamine (TEA) (12.6 mmol) and 2.0 mL trifluoroacetic acid ethyl ester (16.8 mmol) dropwise under argon atmosphere at room temperature. The reaction mixture was stirred for 2 h, and then the mixture was diluted with 20 mL ethyl acetate and 20 mL water. The organic layer was separated, and the aqueous layer was extracted with ethyl acetate. The combined organic layers were washed with saturated sodium chloride and dried over anhydrous sodium sulfate. After evaporation of the solvents under vacuum, the crude product was purified by column chromatography with ethyl acetate/cyclohexane (1:2) as an eluent, and the product was obtained as white crystals (2.5 g, 10.7 mmol, yield 85%). Mp 75–76 °C. ^{1}H NMR (DMSO-d_6) δ: 4.38 (d, *J* = 6.0 Hz, 2H, –CH_2NH–), 4.49 (s, 2H, –CH_2-OH), 5.21 (s, 1H, -OH), 7.13–7.32 (m, 4H, Ar), 10.00 (broad s, 1H, –N*H*-CO–) ppm. ^{13}C NMR (100 MHz, DMSO-d_6) δ: 156.9, 143.3, 137.8, 128.7, 126.2, 125.9, 116.5, 63.2, 43.1. IR (KBr): 3436, 3287, 1636, 1558, 1178 cm^{-1}. MS (ESI): *m*/*z* 256.1 (M+Na)$^+$. HRMS (ESI): *m*/*z* calcd for $C_{10}H_{10}F_3NO_2$ (M+H)$^+$ 234.0742, found 234.0745.

4.1.3. *N*-(3-(((2-Amino-9H-purin-6-yl)oxy)methyl)benzyl)-2,2,2-trifluoroacetamide (3)

To a solution of **7** (1.18 g, 5.0 mmol) in 20 mL anhydrous DMF was added 1.2 g potassium *t*-butoxide (10.7 mmol) followed by 600 mg **2** (2.36 mmol) under an argon atmosphere. The reaction mixture was stirred for 4 h, and then 440 μL glacial acetic acid in 14 mL water was added to neutralize the excess potassium *t*-butoxide. The mixture was diluted with 30 mL ethyl acetate and 30 mL saturated ammonium chloride. The organic layer was separated, and the aqueous layer was extracted twice with ethyl acetate. The combined organic layers were dried over anhydrous sodium sulfate and concentrated under vacuum. The crude product was purified by column chromatography, eluted first with methanol/dichloromethane (1:50) followed by methanol/dichloromethane (1:10), and the product was obtained as a white solid (450 mg, 1.2 mmol, yield 51%). Mp 220–222 °C. ^{1}H NMR (DMSO-d_6) δ: 4.42 (d, *J* = 5.6 Hz, 2H, –CH_2-NH–), 5.49 (s, 2H, –O-CH_2–), 6.30 (s, 2H, –NH_2), 7.27–7.44 (m, 4H, Ar), 7.80 (s, 1H, H8), 10.02 (broad s, 1H, –N*H*-CO–), 12.43 (broad s, 1H, H9) ppm. ^{13}C NMR (100 MHz, DMSO-d_6) δ: 160.1, 156.9, 143.3, 138.2, 137.6, 129.1, 128.7, 127.9, 127.5, 126.4, 126.2, 125.9, 116.5, 67.1, 43.0. IR (KBr): 3467, 1635, 1508, 1401, 1154 cm^{-1}. MS (ESI): *m*/*z* (M+H)$^+$ 367.1. HRMS (ESI): *m*/*z* calcd for $C_{15}H_{13}F_3N_6O_2$ (M+H)$^+$ 367.1130, found 367.1134.

4.1.4. O^6-[3-(Aminomethyl)benzyl]guanine (4)

Compound **3** (300 mg, 0.82 mmol) was suspended in 34 mL methanol along with 2 mL water containing 600 mg anhydrous potassium carbonate (4.34 mmol), and the reaction mixture was heated to reflux for 2 h. After evaporation of the solvents under vacuum, the crude product was purified by column chromatography with methanol/dichloromethane/TEA (1:5:0.05) as an eluent, and the product was obtained as a white solid (170 mg, 0.63 mmol, yield 77%). Mp 159–160 °C. ^{1}H NMR (DMSO-d_6) δ: 3.97 (s, 2H, –CH_2-NH_2), 5.49 (s, 2H, –O-CH_2–), 6.29 (s, 2H, –NH_2), 7.45–7.55 (m, 4H, Ar), 7.83 (s, 1H, H8) ppm, neither are the guanine H9 proton nor the benzylic amine protons observed. ^{13}C NMR (100 MHz, DMSO-d_6) δ: 160.1, 159.9, 157.7, 138.9, 137.3, 135.5, 135.4, 129.2, 129.0, 127.0, 116.2, 66.8, 46.1. IR (KBr): 3446, 1635, 1508, 1400 cm^{-1}. MS (ESI): *m*/*z* 271.1 (M+H)$^+$. HRMS (ESI): *m*/*z* calcd for $C_{13}H_{14}N_6O$ (M+H)$^+$ 271.1307, found 271.1304.

4.1.5. 1-(3-(((2-Amino-9H-purin-6-yl)oxy)methyl)benzyl)-3-(2-chloroethyl)urea (5)

To a solution of **4** (100 mg, 0.37 mmol) in 5 mL DMF was added 0.032 mL 2-chloroethyl isocyanate (0.37 mmol) in 5 mL DMF dropwise at 0 °C, then the reaction mixture was stirred for 2 h at room temperature. The reaction mixture was poured into 20 mL water and extracted twice with 20 mL ethyl acetate. The combined organic layers were dried over anhydrous sodium sulfate and concentrated under vacuum to provide a crude product, which was reprecipitated from methanol to give 115 mg of compound **5** (0.31 mmol, yield 84%) as a white solid. Mp 150–152 °C. ^{1}H NMR (DMSO-d_6) δ: 3.31–3.72 (m, 4H, –CH_2-CH_2-Cl), 4.22 (d, *J* = 6.0 Hz, 2H, –CH_2-NH–), 5.50 (s, 2H, –O-CH_2–), 6.28 (s, 1H, –CO-N*H*–), 6.62 (s, 1H, –N*H*-CO–), 7.23–7.43 (m, 4H, Ar), 7.94 (s, 1H, H8) ppm, the guanine H9 proton was not observed. ^{13}C NMR (100 MHz, DMSO-d_6) δ: 159.9, 159.8, 158.4, 156.1, 154.2, 141.5, 139.3, 136.9, 128.8, 127.6, 127.5, 127.2, 67.6, 45.0, 43.3, 42.0. IR (KBr): 3446, 1635, 1508, 1399 cm^{-1}. MS (ESI): *m*/*z* 375.9 (M+H)$^+$ with ^{35}Cl, 377.9 [M+H]$^+$ with ^{37}Cl. HRMS (ESI): *m*/*z* calcd for $C_{16}H_{18}ClN_7O_2$ (M+H)$^+$ 376.1289, found 376.1284.

4.1.6. 3-(3-(((2-Amino-9H-purin-6-yl)oxy)methyl)benzyl)-1-(2-chloroethyl)-1-nitrosourea (6)

To a solution of **5** (100 mg, 0.27 mmol) in 3 mL anhydrous acetonitrile containing 23.2 μL glacial acetic acid (0.405 mmol) was added 47.3 mg nitrosonium tetrafluoroborate (0.405 mmol), and the reaction mixture was stirred for 3 h at 0 °C until disappearance of the starting material as monitored by TLC. The reaction mixture was poured into 30 mL ice-cold water and extracted twice with 30 mL ice-cold ethyl acetate. The combined organic layers were washed with saturated sodium chloride, dried over anhydrous sodium sulfate and concentrated under vacuum below 30 °C. The crude product was purified by column chromatography with ethyl acetate/petroleum ether (5:1) as an eluent to give the final product **6** (66 mg, 0.16 mmol, yield 59%). Mp 135–137 °C. ^{1}H NMR (DMSO-d_6) δ: 3.31–3.59 (m, 4H, –CH_2-CH_2-Cl), 4.23 (d, *J* = 5.6 Hz, 2H, –CH_2-NH–), 5.50 (s, 2H, –O-CH_2–), 6.43 (s, 2H, –NH_2), 6.97–7.36 (m, 4H, Ar), 7.96 (s, 1H, H8), 9.18 (s, 1H, –N*H*-CO–). ^{13}C NMR (100 MHz, DMSO-d_6) δ: 153.7, 152.3, 137.1, 135.7, 129.2, 129.1, 128.1, 128.0, 127.8, 127.6, 127.4, 67.8, 43.3, 43.2, 42.7. IR (KBr): 3447, 1635, 1507, 1400 cm^{-1}. MS (ESI): *m*/*z* 404.9 [M+H]$^+$ with ^{35}Cl, 406.9 (M+H)$^+$ with ^{37}Cl. HRMS (ESI): *m*/*z* calcd for $C_{16}H_{17}ClN_8O_3$ (M+H)$^+$ 405.1190, found 405.1194.

4.2. Stability

The degradation of **6** was monitored using a Thermo Finnigan HPLC system (Thermo Finnigan, San Jose, CA) interfaced with a diode array detector and an autosampler. The analytes were separated using a Phenomenex Luna C18 reverse phase column (5 μm, 250 × 4.6 mm, Phenomenex, Torrance, CA) eluted with 50% 50 mM ammonium acetate (pH 4.5, solvent A) and 50% methanol (solvent B) at a flow rate of 1.0 mL/min. Compound **6** was dissolved in a minimum volume of dimethyl sulfoxide (DMSO) and diluted with PBS (8 g NaCl, 0.2 g KCl, 1.44 g Na_2HPO_4 and 0.24 g KH_2PO_4 dissolved in 1000 mL deionized water, pH 7.4) or MEM-EBSS supplemented with 10% fetal bovine serum (FBS) and antibiotics (100 U/mL penicillin and 100 μg/mL streptomycin) to give a final concentration of 0.1 mM. The mixtures were incubated at 37 °C with a circulating water bath, and 200 μL of solution was removed at the indicated time point and stored at −20 °C until HPLC analysis. In PBS, all of the samples were injected for HPLC-UV analysis without further treatments. In MEM-EBSS, the cellular and medium components in the samples were precipitated by adding an equal volume of acetonitrile followed by centrifugation at 12,000 rpm for 5 min. The supernatants were removed for HPLC-UV analysis.

4.3. Cell culture

The human glioma SF126 (mer^-, low or no AGT activity), SF767 (mer^+, 61 fmol/10^6 cells) and SF763 (mer^+, 119 fmol/10^6 cells)[39,40] cells were obtained from Peking Union Medical College and were maintained in MEM-EBSS supplemented with 10% FBS and antibiotics (100 U/mL penicillin and 100 μg/mL streptomycin) at 37 °C in a humidified atmosphere of 5% CO_2/95% air. The cells were passaged as required every 2–3 days.

4.4. Cell survival assay

The cell survival assay was performed using the Cell Counting Kit-8 (CCK8, Dojindo China CO., Ltd, Shanghai, China) in 96-well plates. Cells were plated at a density of 5000 cells/well in 96-well plates and allowed to grow for 24 h. Then, the medium was discarded and replaced with fresh medium containing different concentrations of drugs for a 24 h incubation. For the combination treatments, O^6-BG was added to give a final concentration of 20 μM and was incubated for 2 h before exposure to ACNU or BCNU. After 2 h, the medium was replaced with fresh medium containing different concentrations of ACNU or BCNU for an additional 24 h. Then, the medium containing different concentrations of drugs was discarded, and 100 μL fresh medium containing 10% CCK8 was added to each well. After incubation for 3 h, the absorbance was determined using a Thermo Scientific Multiskan FC (Waltham, MA) at 450 nm. The cell survival rate (%) was expressed by the following formula:

$$\text{Survival rate}(\%) = (A_{drug} - A_{blank})/(A_{control} - A_{blank}) \times 100\%.$$

where A_{drug} represents the absorbance of the wells containing the medium, cells and drug, A_{blank} represents the absorbance of the wells containing only the medium, and $A_{control}$ represents the absorbance of the wells containing the medium and cells. The results were expressed as the mean values ± standard deviation (SD) from at least three independent experiments. The final concentration of ethanol (BCNU was dissolved in ethanol) or DMSO (**6** and O^6-BG was dissolved in DMSO) in culture medium was below 0.1%.

4.5. In vitro treatment of calf thymus DNA with 6

Calf thymus DNA (CT DNA) was dissolved in phosphate buffered saline (10 mM Tris, 50 mM NaCl, 50 mM Na_2HPO_4, pH 7.4) with a final concentration of 1 mg/mL. A freshly prepared solution of **6** (dissolved in DMSO) was added to the CT DNA solution to give a final concentration of 0.1, 0.2, and 0.4 mM. The reaction mixture was incubated at 37 °C with a circulating water bath for 12 h. Aliquots of 400 μL of reaction solution were removed for DNA isolation. For each sample, the DNA was precipitated by the addition of 800 μL ice-cold ethanol followed by centrifugation at 12,000 rpm for 5 min at 4 °C. The resulting DNA pellets were washed with 1 mL of 75% ethanol and then with 1 mL of 100% ethanol. All DNA samples were dried under a nitrogen stream and stored at −20 °C until enzymatic hydrolysis. The CT DNA samples treated with ACNU (dissolved in deionized water) and BCNU (dissolved in ethanol) were regarded as positive controls. The negative control DNA samples were incubated under the same conditions as the treated DNA samples, except without the addition of drugs.

4.6. Treatment of human glioma SF763 cells with 6

The human glioma SF763 cells were plated at a density of 10^6 cells in T75 culture flasks and were allowed to grow to reach ~90% confluence. Then, the medium was discarded and replaced with freshly prepared medium containing different concentrations of **6** (0.1, 0.2, and 0.4 mM). After incubation for 12 h, the medium was discarded, and the cells were washed twice with D-Hanks' basal salt solution. The cells were digested with 0.25% trypsin containing 0.02% versene and collected by centrifugation at 1000 rpm for 10 min. All cell samples were stored at −20 °C until DNA isolation. The cells treated with ACNU and BCNU were regarded as positive controls. The negative control cell samples were incubated under the same conditions as the treated cell samples, except without the addition of drugs.

4.7. DNA isolation

DNA was isolated from cells using the procedure previously described with some modifications.[22,46,47] Briefly, the cell samples were suspended in 10 mL cell lysis buffer (10 mM Tris–HCl, 0.1 M EDTA, and 0.5% SDS, pH 8.0), then 70 μL protease K (21 U) and 100 μL RNase A (0.5 mg) were added. The mixture was incubated at 37 °C overnight with shaking followed by a standard phenol–chloroform extraction procedure. The supernatant containing DNA was collected, and an equal volume of ice-cold isopropanol was added to precipitate DNA. After centrifugation at 12,000 rpm for 10 min, the DNA pellets were washed with 1 mL of 75% ethanol and then with 1 mL of 100% ethanol. All DNA samples were dried under a nitrogen stream and stored at −20 °C until enzymatic hydrolysis.

4.8. DNA enzymatic hydrolysis

The DNA enzymatic hydrolysis was performed as previously described with some modifications.[22,44] DNA samples were redissolved in Tris–HCl buffer (10 mM, pH 7.4). The purity of the isolated DNA samples from SF763 cells was determined by the absorbance ratio A260/A280, which was typically between 1.7 and 2.0. Four enzymes, including recombinant deoxyribonuclease I (DNaseI), S1 nuclease, alkaline phosphatase (CIAP, from calf intestine), and phosphodiesterase I (from *Crotalus adamanteus* venom), were used to digest DNA into single nucleotides. Briefly, a solution of 100 μL DNA was spiked with $^{15}N_3$-dG–dC internal standard, and the mixture was heated at 98 °C for 5 min followed quickly by chilling in an ice-bath for 10 min. Then, 15 μL DNase I (3 U/μL) and

10 μL S1 nuclease (10 U/μL) were added for incubation at 37 °C for 6 h. Subsequently, 20 μL CIAP (1 U/μL) and 5 μL phosphodiesterase I (0.001 U/μL) were further added to the mixture for incubation at 37 °C overnight. Finally, enzymes and undigested DNA were removed by a Microcon YM-10 molecular weight centrifugal filter (Billerica, MA). The final concentration of the $^{15}N_3$-dG–dC internal standard in the filtrate was 9.6 nM. A 10 μL aliquot was removed for dGuo quantitation, and approximately 140 μL of filtrate remained for HPLC–ESI-MS/MS analysis.

4.9. dGuo quantitation

The DNA concentration was quantified by HPLC-UV analysis for dGuo in the enzymatic hydrolysates. The quantitation of dGuo was conducted using a Thermo Finnigan HPLC system (Thermo Finnigan, San Jose, CA) incorporating a diode array detector and an autosampler. A Phenomenex Luna C18 reverse phase column (5 μm, 250 × 4.6 mm, Phenomenex, Torrance, CA) was used for dGuo separation with deionized water (solvent A) and methanol (solvent B) as the mobile phases at a flow rate of 0.7 mL/min. The gradient elution was performed as previously described.[22] The UV wavelength was monitored at 254 nm. The quantitation was based on the HPLC peak area of dGuo using an external calibration curve constructed by plotting the HPLC peak area of the dGuo standard versus the corresponding concentration.

4.10. HPLC–ESI-MS/MS analysis of dG–dC cross-links

The quantitation of dG–dC cross-links in DNA enzymatic hydrolysates was performed using a Thermo TSQ Quantum Discovery MAX triple quadrupole mass spectrometer (Thermo Finnigan, San Jose, CA) interfaced with an HPLC system. A Zorbax SB C18 reverse phase column (2.1 × 150 mm, 5 μm particle size; Agilent Technologies, Palo Alto, CA) was eluted with deionized water containing 0.01% acetic acid (solvent A) and acetonitrile (solvent B) at a flow rate of 0.2 mL/min. The solvent composition was maintained with 5% B at 0 min and then linearly increased to 10% B in 23 min. Subsequently, solvent B was decreased to 5% over 2 min followed by a 10 min equilibration. Enzymatic hydrolysate (15 μL) was injected for HPLC–ESI-MS/MS analysis. The mass spectrometer parameters were optimized using the $^{15}N_3$-dG–dC internal standard. The ESI source was operated in the positive ion mode with argon as the collision gas (1.5 mTorr). Nitrogen was used as the sheath gas (50 psi) and the auxiliary gas (5 psi). The spray voltage was 3.5 kV, and the capillary temperature was 300 °C. The tube lens offset, source collision induced dissociation (CID) and collision energy were set at 121 V, 10 V and 20 eV, respectively. The SRM mode was used for quantitative analysis of dG–dC cross-links by monitoring the transitions of m/z 521 → 289 for dG–dC and m/z 524 → 292 for the $^{15}N_3$-dG–dC internal standard. The levels of dG–dC cross-link were expressed as fmol of dG–dC per mg DNA. The amount of DNA was calculated from the dGuo content by considering that 1 mg of DNA contains 3 μmol of nucleotides and that dGuo accounts for 22% of the total nucleotides in DNA.[48,49] The results were expressed as the mean values ± standard deviation (SD) from triplicate experiments.

4.11. Molecular docking study

Two X-ray crystal structures of the AGT protein with PDB entry 1T39 and 1QNT were used as templates to model a new AGT crystal structure (NCBI Reference Sequence: NP_002403.2) using the MODELER section in Discovery Studio 4.0 (Accelrys Inc.). The conformational rationality of the modeled AGT protein was evaluated by the Ramanchandran Plot and the Line Plot shown in Figures S3 and S4, respectively, in the Supplementary materials. GOLD Suite 5.2 software (Cambridge Structural Database System) was selected for the docking simulations. Self-docking was performed to validate the docking method using the X-ray crystal structure of human AGT with PDB entry 1T38 (3.2 Å resolution) bound to DNA containing O^6-MG as the protein–ligand crystal complex model. For self-docking, DNA was removed, except for O^6-MG, which was used as the native ligand for self-docking. Solvent molecules were removed in the X-ray crystal structure of 1T38. Geometry optimizations of the ligands were performed at the B3LYP/6-31g+(d,p) theoretical level using Gaussian 09 software (Gaussian Inc., Wallingford, CT, USA).[50] Hydrogen atoms were added to the modeled protein, and the Gold score was selected as the scoring function.

Acknowledgments

The authors would like to thank Dr. Stephen S. Hecht in the University of Minnesota for his valuable suggestions to the study. This study was supported by grants from the National Natural Science Foundation of China (No. 21277001), Natural Science Foundation of Beijing (No. 7162015), Beijing Municipal Education Commission Science and Technology Project (No. PXM2015_014204_500175), and the Jinghua Talent Project of Beijing University of Technology (015000514115001).

A. Supplementary data

Supplementary data associated with this article can be found, in the online version, at http://dx.doi.org/10.1016/j.bmc.2016.03.041.

References and notes

1. Gnewuch, C. T.; Sosnovsky, G. *Chem. Rev.* **1997**, *97*, 829.
2. Rajski, S. R.; Williams, R. M. *Chem. Rev.* **1998**, *98*, 2723.
3. Frenay, M. P.; Fontaine, D.; Vandenbos, F.; Lebrun, C. *Eur. J. Neurol.* **2005**, *12*, 685.
4. Jenkinson, M. D.; Smith, T. S.; Haylock, B.; Husband, D.; Shenoy, A.; Vinjamuri, S.; Walker, C.; Pietronigro, D.; Warnke, P. C. *J. Neuro-Oncol.* **2010**, *99*, 103.
5. Bodell, W. J. *J. Neuro-Oncol.* **2009**, *91*, 257.
6. Muniandy, P. A.; Liu, J.; Majumdar, A.; Liu, S. T.; Seidman, M. M. *Crit. Rev. Biochem. Mol. Biol.* **2010**, *45*, 23.
7. Deans, A. J.; West, S. C. *Nat. Rev. Cancer* **2011**, *11*, 467.
8. Zhao, L. J.; Ma, X. Y.; Zhong, R. G. *J. Phys. Org. Chem.* **2012**, *25*, 1153.
9. Zhao, L. J.; Ma, X. Y.; Zhong, R. G. *Int. J. Quantum Chem.* **2013**, *113*, 1299.
10. Pegg, A. E. *Cancer Res.* **1990**, *50*, 6119.
11. Limp-Foster, M.; Kelley, M. R. *Environ. Mol. Mutagen.* **2000**, *35*, 71.
12. Kokkinakis, D. M.; Bocangel, D. B.; Schold, S. C.; Moschel, R. C.; Pegg, A. E. *Clin. Cancer Res.* **2001**, *7*, 421.
13. Bacolod, M. D.; Johnson, S. P.; Ali-Osman, F.; Modrich, P.; Bullock, N. S.; Colvin, O. M.; Bigner, D. D.; Friedman, H. S. *Mol. Cancer Ther.* **2002**, *1*, 727.
14. Ishiguro, K.; Zhu, Y. L.; Shyam, K.; Penketh, P. G.; Baumann, R. P.; Sartorelli, A. C. *Biochem. Pharmacol.* **2010**, *80*, 1317.
15. Pegg, A. E. *Chem. Res. Toxicol.* **2011**, *24*, 618.
16. Srivenugopal, K. S.; Yuan, X. H.; Friedman, H. S.; AliOsman, F. *Biochemistry* **1996**, *35*, 1328.
17. Xu-Welliver, M.; Pegg, A. E. *Carcinogenesis* **2002**, *23*, 823.
18. Bodell, W. J.; Rupniak, H. T. R.; Rasmussen, J.; Morgan, W. F.; Rosenblum, M. L. *Cancer Res.* **1984**, *44*, 3763.
19. Srivenugopal, K. S. *Biochem. Pharmacol.* **1992**, *43*, 1159.
20. Beith, J.; Hartley, J.; Darling, J.; Souhami, R. *Br. J. Cancer* **1997**, *75*, 500.
21. Bodell, W. J. *Cancer Res.* **2003**, *522*, 85.
22. Sun, G. H.; Zhao, L. J.; Fan, T. J.; Li, S. S.; Zhong, R. G. *Chem. Res. Toxicol.* **2014**, *27*, 1253.
23. Pegg, A. E.; Chung, L.; Moschel, R. C. *Biochem. Pharmacol.* **1997**, *53*, 1559.
24. Dolan, M. E.; Roy, S. K.; Garbiras, B. J.; Helft, P.; Paras, P.; Chae, M. Y.; Moschel, R. C.; Pegg, A. E. *Biochem. Pharmacol.* **1998**, *55*, 1701.
25. Griffin, R. J.; Arris, C. E.; Bleasdale, C.; Boyle, F. T.; Calvert, A. H.; Curtin, N. J.; Dalby, C.; Kanugula, S.; Lembicz, N. K.; Newell, D. R.; Pegg, A. E.; Golding, B. T. *J. Med. Chem.* **2000**, *43*, 4071.
26. Kaina, B.; Muhlhausen, U.; Piee-Staffa, A.; Christmann, M.; Boy, R. G.; Rosch, F.; Schirrmacher, R. *J. Pharmacol. Exp. Ther.* **2004**, *311*, 585.
27. Nelson, M. E.; Loktionova, N. A.; Pegg, A. E.; Moschel, R. C. *J. Med. Chem.* **2004**, *47*, 3887.
28. Wei, G. P.; Loktionova, N. A.; Pegg, A. E.; Moschel, R. C. *J. Med. Chem.* **2005**, *48*, 256.
29. Javanmard, S.; Loktionova, N. A.; Fang, Q.; Pauly, G. T.; Pegg, A. E.; Moschel, R. C. *J. Med. Chem.* **2007**, *50*, 5193.

30. Pauly, G. T.; Loktionova, N. A.; Fang, Q. M.; Vankayala, S. L.; Guida, W. C.; Pegg, A. E. *J. Med. Chem.* **2008**, *51*, 7144.
31. Schilsky, R. L.; Dolan, M. E.; Bertucci, D.; Ewesuedo, R. B.; Vogelzang, N. J.; Mani, S.; Wilson, L. R.; Ratain, M. J. *Clin. Cancer Res.* **2000**, *6*, 3025.
32. Quinn, J. A.; Pluda, J.; Dolan, M. E.; Delaney, S.; Kaplan, R.; Rich, J. N.; Friedman, A. H.; Reardon, D. A.; Sampson, J. H.; Colvin, O. M.; Haglund, M. M.; Pegg, A. E.; Moschel, R. C.; McLendon, R. E.; Provenzale, J. M.; Gururangan, S.; Tourt-Uhlig, S.; Herndon, J. E.; Bigner, D. D.; Friedman, H. S. *J. Clin. Oncol.* **2002**, *20*, 2277.
33. Gajewski, T. F.; Sosman, J.; Gerson, S. L.; Liu, L. L.; Dolan, E.; Lin, S.; Vokes, E. E. *Clin. Cancer Res.* **2005**, *11*, 7861.
34. Quinn, J. A.; Jiang, S. X.; Reardon, D. A.; Desjardins, A.; Vredenburgh, J. J.; Rich, J. N.; Gururangan, S.; Friedman, A. H.; Bigner, D. D.; Sampson, J. H.; McLendon, R. E.; Herndon, J. E.; Walker, A.; Friedman, H. S. *J. Clin. Oncol.* **2009**, *27*, 1262.
35. Qiu, Q. Y.; Dudouit, F.; Banerjee, R.; McNamee, J. P.; Jean-Claude, B. J. *Prostate* **2004**, *59*, 13.
36. Qiu, Q. Y.; Domarkas, J.; Banerjee, R.; Merayo, N.; Brahimi, F.; McNamee, J. P.; Gibbs, B. F.; Jean-Claude, B. J. *Clin. Cancer Res.* **2007**, *13*, 331.
37. Mineura, K.; Fukuchi, M.; Kowada, M.; Terashima, I.; Kohda, K. *Int. J. Cancer* **1995**, *63*, 148.
38. Wiencke, J. K.; Wiemels, J. *Mutat. Res. Rev. Genet. Toxicol.* **1995**, *339*, 91.
39. Aida, T.; Bodell, W. J. *Cancer Res.* **1987**, *47*, 1361.
40. Bobola, M. S.; Blank, A.; Berger, M. S.; Silber, J. R. *Mol. Carcinog.* **1995**, *13*, 70.
41. Zhao, L. J.; Li, L. L.; Xu, J.; Zhong, R. G. *Int. J. Mass Spectrom.* **2014**, *368*, 30.
42. Li, L. L.; Zhao, L. J.; Zhong, R. G. *Rapid Commun. Mass Spectrom.* **2014**, *28*, 439.
43. Bodell, W. J.; Pongracz, K. *Chem. Res. Toxicol.* **1993**, *6*, 434.
44. Bai, B. Q.; Zhao, L. J.; Zhong, R. G. *Rapid Commun. Mass Spectrom.* **2011**, *25*, 2027.
45. Keppler, A.; Gendreizig, S.; Gronemeyer, T.; Pick, H.; Vogel, H.; Johnsson, K. *Nat. Biotechnol.* **2003**, *21*, 86.
46. Cao, H. C.; Hearst, J. E.; Corash, L.; Wang, Y. S. *Anal. Chem.* **2008**, *80*, 2932.
47. Michaelson-Richie, E. D.; Ming, X.; Codreanu, S. G.; Loeber, R. L.; Liebler, D. C.; Campbell, C.; Tretyakova, N. Y. *J. Proteome Res.* **2011**, *10*, 2785.
48. Gupta, R. C. *Cancer Res.* **1985**, *45*, 5656.
49. Zhao, L. J.; Balbo, S.; Wang, M. Y.; Upadhyaya, P.; Khariwala, S. S.; Villalta, P. W.; Hecht, S. S. *Chem. Res. Toxicol.* **2013**, *26*, 1526.
50. Frisch, M. J.; Trucks, G. W.; Schlegel, H. B.; Scuseria, G. E.; Robb, M. A.; Cheeseman, J. R.; Scalmani, G.; Barone, V.; Mennucci, B.; Petersson, G. A.; Nakatsuji, H.; Caricato, M.; Li, X.; Hratchian, H. P.; Izmaylov, A. F.; Bloino, J.; Zheng, G.; Sonnenberg, J. L.; Hada, M.; Ehara, M.; Toyota, K.; Fukuda, R.; Hasegawa, J.; Ishida, M.; Nakajima, T.; Honda, Y.; Kitao, O.; Nakai, H.; Vreven, T.; Montgomery, J. A.; Peralta, J. E.; Ogliaro, F.; Bearpark, M.; Heyd, J. J.; Brothers, E.; Kudin, K. N.; Staroverov, V. N.; Kobayashi, R.; Normand, J.; Raghavachari, K.; Rendell, A.; Burant, J. C.; Iyengar, S. S.; Tomasi, J.; Cossi, M.; Rega, N.; Millam, N. J.; Klene, M.; Knox, J. E.; Cross, J. B.; Bakken, V.; Adamo, C.; Jaramillo, J.; Gomperts, R.; Stratmann, R. E.; Yazyev, O.; Austin, A. J.; Cammi, R.; Pomelli, C.; Ochterski, J. W.; Martin, R. L.; Morokuma, K.; Zakrzewski, V. G.; Voth, G. A.; Salvador, P.; Dannenberg, J. J.; Dapprich, S.; Daniels, A. D.; Farkas, Ö.; Foresman, J. B.; Ortiz, J. V.; Cioslowski, J.; Fox, D. J. *Gaussian 09, Revision A.01*; Gaussian Inc.: Wallingford, CT, 2009.